MOLECULAR DOCKING OF VARIOUS CHALCONE ANALOGUES FOR THEIR ANTIHYPERLIPIDEMIC ACTIVITY USING MOLEGRO VIRTUAL DOCKER

Abstract

A high quantity of fat particles (lipids) in the blood is a disorder known as hyperlipidemia. Antihyperlipidemic drugs work to enhance HDL cholesterol, while others work to lower triglyceride levels and low-density lipoprotein cholesterol levels. In this paper, we investigate many substituted chalcone analogs. Using the Molegro virtual Docker program, we analyze the docking experiments of the substituted chalcone analogus as the anti-hyperlipidemic drug in this study. Out of 650 compounds, our research found that over 10 compounds had substantial binding affinities with five different types of proteins. The five different protein receptor types 1EZF, 1OSH, 2ZNN, 2ZNQ, and 3LD6 each demonstrated strong binding affinity for the substances 444, 419, 380, 366, and 234. Researchers can create another powerful chemical that acts as an anti-hyperlipidemic drug using docking experiments.

Keywords: Molegro Virtual, Docker, RCSB HDL, 3D structure

Authors

Hemlata Mahant
Faculty
Department of Pharmaceutical Sciences
Shri Shankaracharya Technical Campus
Junwani, Bhilai, India.

Gitanjali Kashyap
Faculty
Department of Pharmaceutical Sciences
Shri Shankaracharya Technical Campus
Junwani, Bhilai, India.

Vinay Sagar Verma
Faculty
Department of Pharmaceutical Sciences
Shri Shankaracharya Technical Campus
Junwani, Bhilai, India.

Achal Mishra
Faculty
Department of Pharmaceutical Sciences
Shri Shankaracharya Technical Campus
Junwani, Bhilai, India.
achal.mishra03@.gmail.com

Copyright © 2024 Authors

I. INTRODUCTION

In addition to performing other important biochemical activities for maintaining the health of the human heart, cholesterol is a key component in the production of membranes.(1) However, atherosclerotic cardiovascular diseases such as coronary heart disease and stroke arise when plasma cholesterol levels rise above what is necessary for these processes.(2) Additionally, hyper-lipidemia may hide the liver and muscle insulin resistance that starts the development of diabetes in patients and cause additional irregularities such as the oxidation of free fatty acids, which results in the creation of ketone bodies.(3) Anti-hyperlipidemic medications work to lower blood lipid levels in various ways.(4) Some try to lower levels of low-density lipoprotein cholesterol, while others lower triglyceride levels, and yet others help boost levels of high-density lipoprotein cholesterol.(5) Modern drug design currently uses the molecular docking technique to study drug-receptor interactions.(6) The literature claims that computational tools can assist in drug design.(7) It can also be used to understand how drugs interact with receptors. In this study we docked Squalene synthase catalyzes, farnesoid X receptor, Peroxisome proliferator-activated receptors (PPARs) alpha, Peroxisome proliferator-activated receptors (PPARs) delta and lanosterol 14alpha-demethylase with derivatives of chalcone analogues as ligand by Molegro Virtual Docker (MVD)(8)

1. **Chalcone:** A chalcone is a basic chemical structure found in a variety of natural plant products, such as teas, vegetables, fruits, and spices. Chalcones, which are members of the flavonoid family and function as biosynthetic intermediaries for flavonoids, have a diverse range of pharmacological targets and structural variability.(9)(10) Members of the Chalcone family have drawn a lot of attention due to their potential for synthetic and biosynthetic production as well as the breadth of their biological activities, which include anticancer, anti-inflammatory, antidiabetic, cancer chemopreventive, antioxidant, antimicrobial, anti-leishmanial, anti-malarial, and antihyperlipidemic effects.(11)(12) More significantly, a number of chalcone compounds have been authorized for use in both clinical and commercial settings for a range of medical disorders.(13) (14)

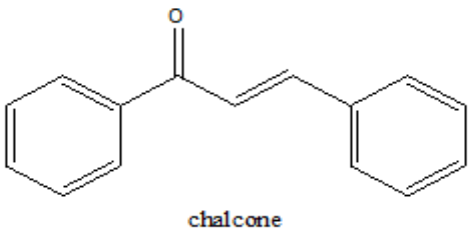

Figure 1: 2D Structure of Chalcone

2. **Molegro Virtual Docker:** We can do docking simulations in a completely integrated computational environment thanks to a program called Molegro Virtual Docker that simulates the docking of proteins and ligands.(15) Numerous different proteins have been successfully docked using MVD, which has performance comparable to that of other docking tools like AutoDock4 and AutoDock Vina.(16) Four native scoring functions and four search algorithms are included in the MVD software.(17) (18)

Copyright © 2024 Authors

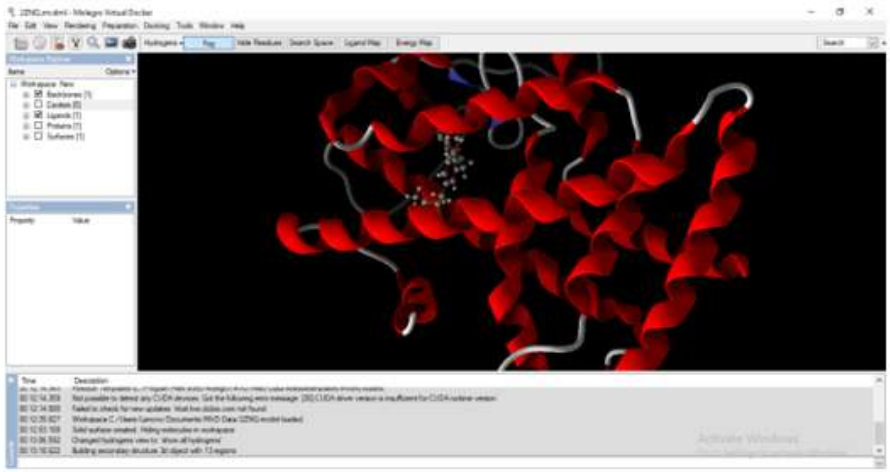

Figure 2: Molegro Virtual Docker 6.0

II. RESULTS

The MolDock Score describes the ability of Chalcone derivatives to bind to targets. The metric for analyzing the docking outcomes is the MolDock Score. The Chalcone Derivatives' MolDock Score, Rerank Score, and Hydrogen Bond Interaction are ranked in that manner. The ligand's posture, which has the lowest MolDcok score, demonstrates a high affinity for its enzyme target. Chalcone derivatives' in silico docking study on Squalene synthase catalyzes¬¬(PDB ID: 1EZF), farnesoid X receptor (PDB ID: 1OSH), Peroxisome proliferator-activated receptors (PPARs)alpha (PDB ID: 2ZNN), Peroxisome proliferator-activated receptors (PPARs) delta (PDB ID: 2ZNQ) and lanosterol 14alpha-demethylase (PDB ID: 3LD6) ranking based on Re-rank Score is represented in Table 2,3,4,5 and 6. The re-rank score was suggested to compare binding affinities, according to the literature. The cutoff score for this software was set at -60 AU. molecule presentations that can get cut-off scores. The binding patterns of the poses are captured using Biovia Visualizer software. docking pose of Chalcone derivatives is represented in Figure

Table 1: Ranking of Ligand and Poses based on Re-Rank Score for Squalene Synthase Catalyzes

Ligand code	Moldock	Re-ran k	Docking	H Bond
444	-118.879	-89.4759	-118.088	-1.81252
586	-110.948	-86.5549	-111.205	0
445	-112.373	-85.4024	-113.471	-1.93558
99	-105.398	-82.3979	-104.97	-1.68423
244	-93.0628	-81.7151	-92.3871	-1.37222
451	-94.9064	-81.3992	-95.2335	0
643	-105.495	-81.1421	-103.937	0
446	-103.897	-81.0609	-102.983	-1.45297
418	-104.313	-80.8477	-112.995	-1.96331
674	-101.554	-80.8459	-100.848	-1.19106
ROSUVASTATIN	-115.354	-74.58	-117.069	-6.62626

Copyright © 2024 Authors

EZELIMIBE	-106.047	-59.6707	-111.311	-6.43995
ATORVASTATIN	-135.523	-56.1164	-132.113	-2.5

Table 2: Ranking of Ligand and Poses based on Re-Rank Score for Farnesoid X Receptor

Ligand code	Moldock	Re-ran k	Docking	H Bond
419	-120.983	-102.951	-83.4149	-0.2694
444	-127.973	-101.576	-109.376	0
233	-123.015	-100.519	-96.967	0
582	-123.821	-98.5686	-82.1567	0
418	-113.617	-98.2649	-88.4015	-1.11672
648	-114.817	-97.9852	-94.2071	0
686	-107.919	-97.3327	-90.2736	-2.42386
366	-115.416	-97.1997	-95.2135	0
472	-113.794	-95.9952	-93.3231	0
487	-110.109	-95.7819	-88.015	-2.76144
ROSUVASTATIN	-126.105	-88.505	-93.3884	-2.26085
EZELIMIBE	-105.989	-48.3069	-103.42	-5.74129
ATORVASTATIN	-101.82	353.338	9923.55	-2.41255

Table 1: Ranking of Ligand and Poses based on Re-rank score for Peroxisome Proliferator-Activated Receptors (PPARs)Alpha

Ligand code	Moldock	Re-ran k	Docking	H Bond
380	-147.552	-121.521	-141.598	0
586	-159.652	-111.438	-154.761	-0.9247
336	-133.77	-111.123	-131.095	-0.2143
557	-145.608	-110.913	-132.302	0
175	-134.568	-109.98	-134.998	0
441	-147.701	-109.975	-147.841	0
179	-140.591	-107.939	-142.698	0
444	-132.671	-107.44	-131.582	0
559	-162.56	-107.191	-151.129	0
328	-127.318	-106.192	-121.473	0
ATORVASTATIN	-184.003	-123.226	-192.426	-4.48156
EZELIMIBE	-143.527	-109.854	-145.443	-4.83029
ROSUVASTATIN	-123.979	-72.9949	-135.193	-2.71965

Table 2: Ranking of Ligand and Poses based on Re-Rank Score for Peroxisome Proliferator-Activated Receptors (PPARs) Delta

Ligand code	Moldock	Re-ran k	Docking	H Bond
366	-147.503	-113.055	-145.968	0
419	-127.51	-107.539	-130.411	-3.10727

Copyright © 2024 Authors

643	-130.216	-107.118	-130.75	0
441	-136.368	-104.797	-136.412	-0.28573
233	-127.989	-104.689	-124.732	0
473	-128.176	-104.666	-128.884	-1.05403
328	-126.872	-103.888	-124.382	0
183	-125.867	-103.311	-123.336	-1.33129
582	-130.586	-102.819	-129	0
42	-125.769	-102.782	-129.467	-1.57916
ROSUVASTATIN	-123.458	-91.626	-123.412	-7.36093
EZELIMIBE	-131.758	-92.3829	-131.533	-7.73417
ATORVASTATIN	-164.557	-122.047	-161.32	-2.33475

Table 3: Ranking of Ligand and Poses based on Re-Rank Score for Lanosterol 14alpha-Demethylase

Ligand code	Moldock	Re-ran k	Docking	H Bond
234	-125.472	-103.515	-128.027	-2.51674
369	-128.249	-101.004	-123.105	-0.33555
441	-126.769	-100.393	-125.574	0
684	-117.64	-100.282	-119.71	-0.12375
588	-118.382	-99.964	-115.651	0
581	-116.856	-99.7643	-116.979	-1.86483
167	-118.175	-99.6777	-120.884	-2.5
380	-128.022	-99.4894	-126.264	-2.42776
419	-119.851	-99.4083	-121.561	-1.63658
445	-120.744	-99.3561	-125.193	-0.30838
ROSUVASTATIN	-123.491	-76.9423	-124.988	-6.53476
EZELIMIBE	-117.424	-82.5165	-131.533	-1.71518
ATORVASTATIN	-149.563	-94.612	-133.755	-3.1509

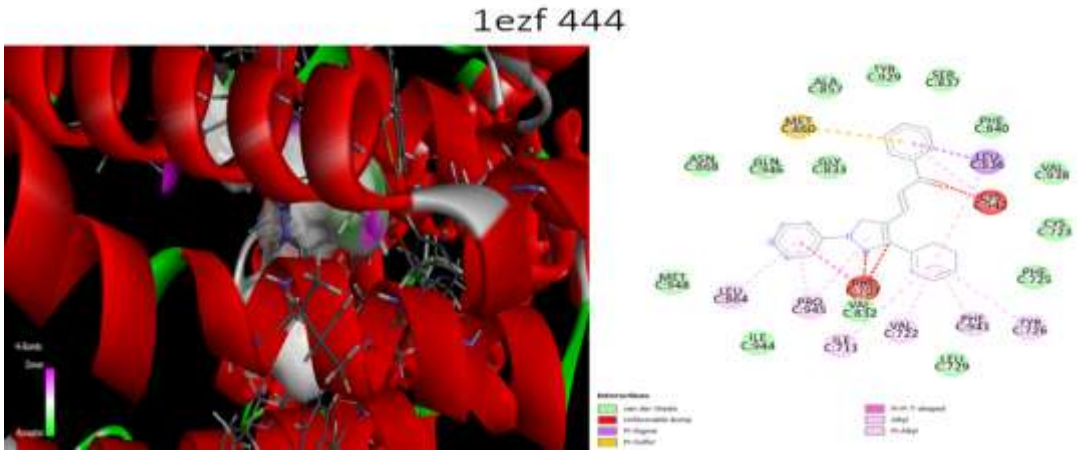

Figure 3: Docking image of the molecule code 444 docked with 1ezf Visualized throuth MVD and Biovia Visualizer software. A) 3D model. B) 2Dpose model.

Copyright © 2024 Authors

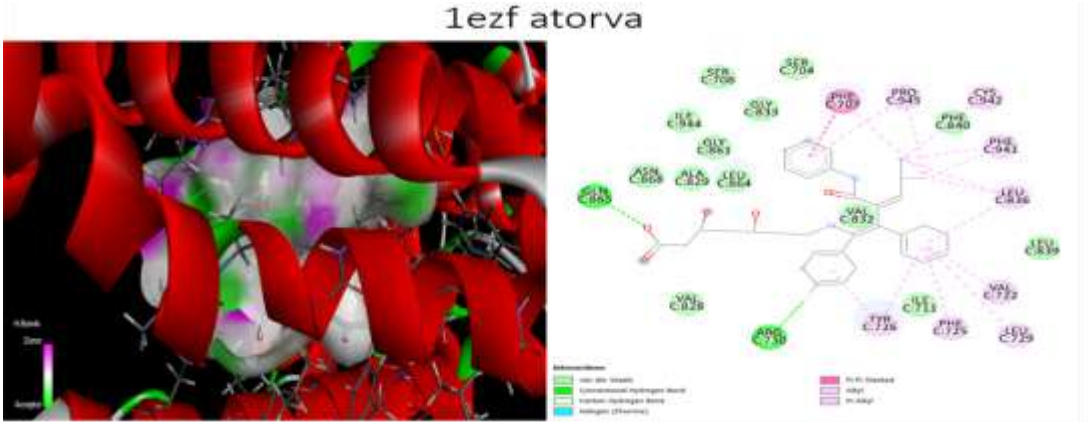

Figure 4: Docking image of the standard molecule Atorvastatin docked with 1ezf Visualized throuth MVD and Biovia Visualizer software. A) 3D model. B) 2Dpose model.

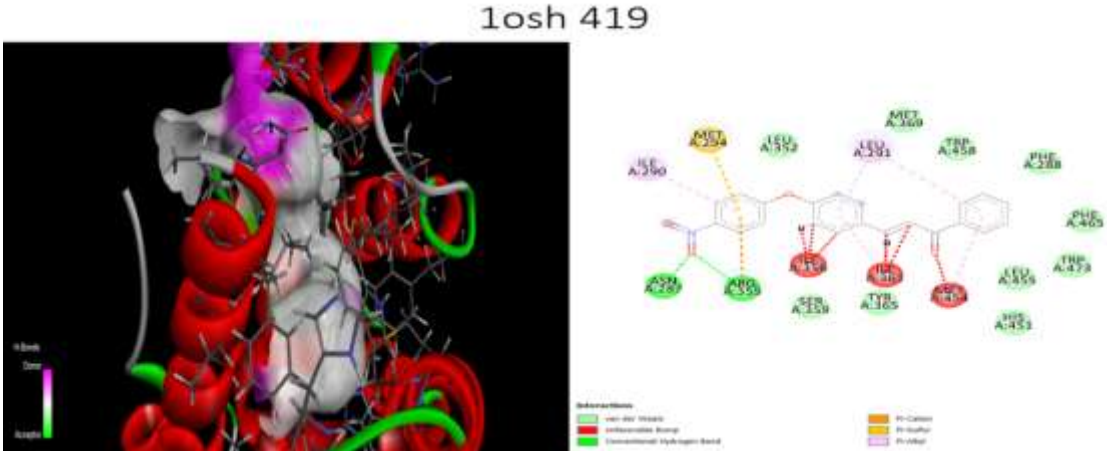

Figure 5: Docking image of the molecule code 419 docked with 1osh Visualized throuth MVD and Biovia Visualizer software. A) 3D model. B) 2Dpose model.

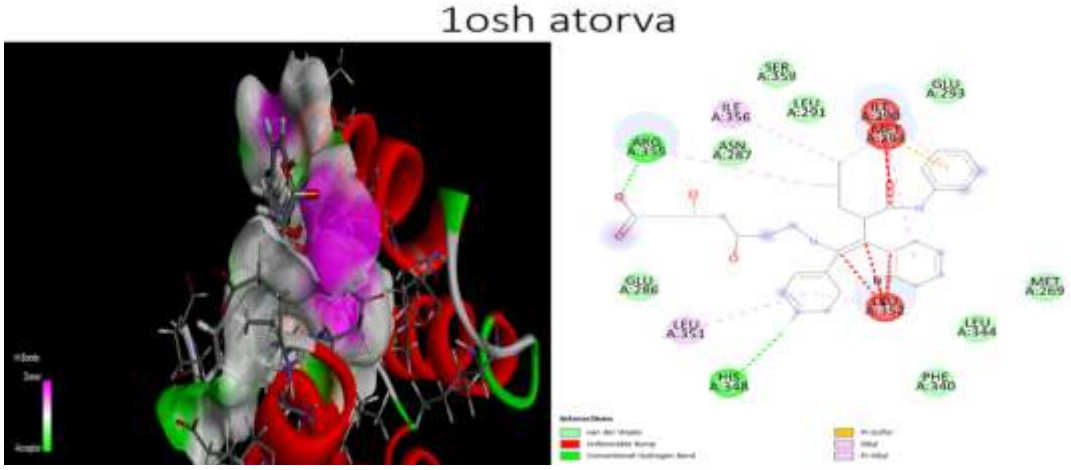

Figure 6: Docking image of the standard molecule Atorvastatin docked with 1osh Visualized throuth MVD and Biovia Visualizer software. A) 3D model. B) 2Dpose model.

Copyright © 2024 Authors

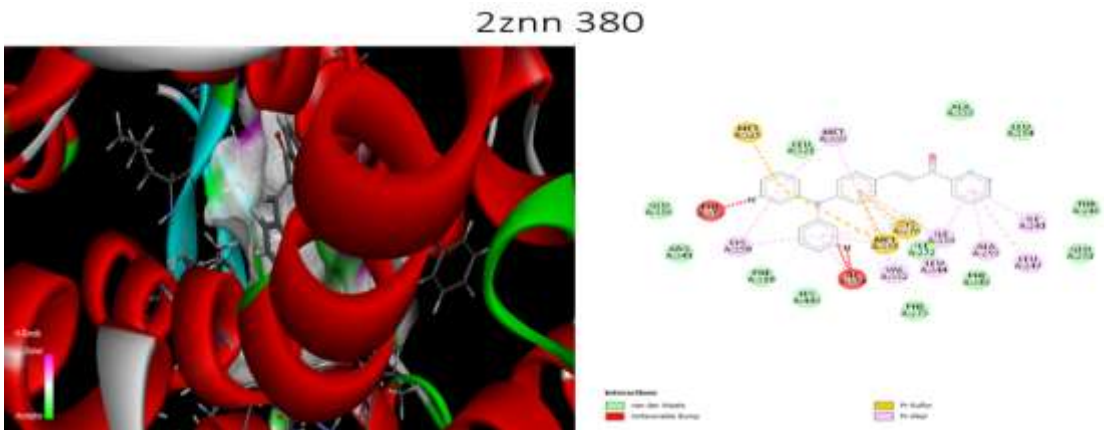

Figure 7: Docking image of the molecule code 380 docked with 2znn Visualized throuth MVD and Biovia Visualizer software. A) 3D model. B) 2Dpose model.

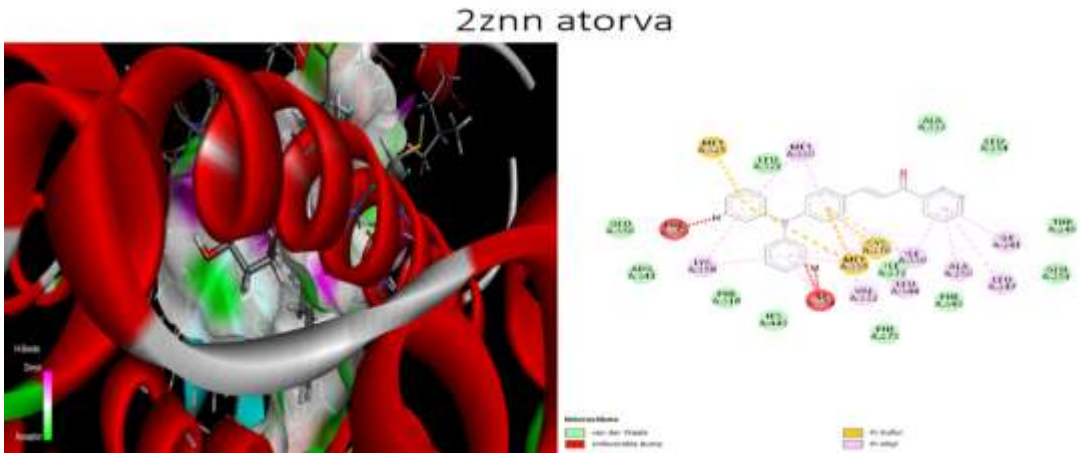

Figure 8: Docking image of the standard molecule Atorvastatin docked with 2znn Visualized throuth MVD and Biovia Visualizer software. A) 3D model. B) 2Dpose model.

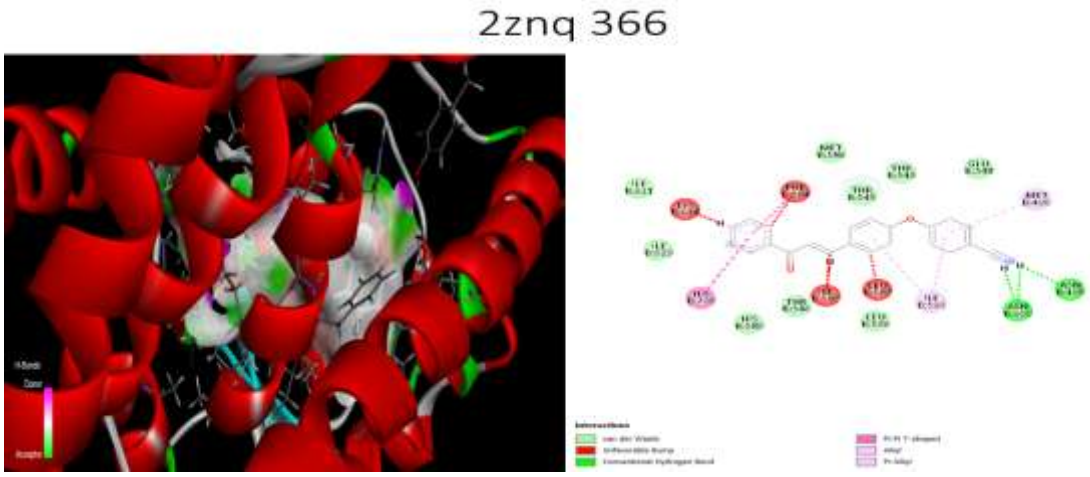

Figure 9: Docking image of the molecule code 366 docked with 2znq Visualized throuth MVD and Biovia Visualizer software. A) 3D model. B) 2Dpose model.

Copyright © 2024 Authors

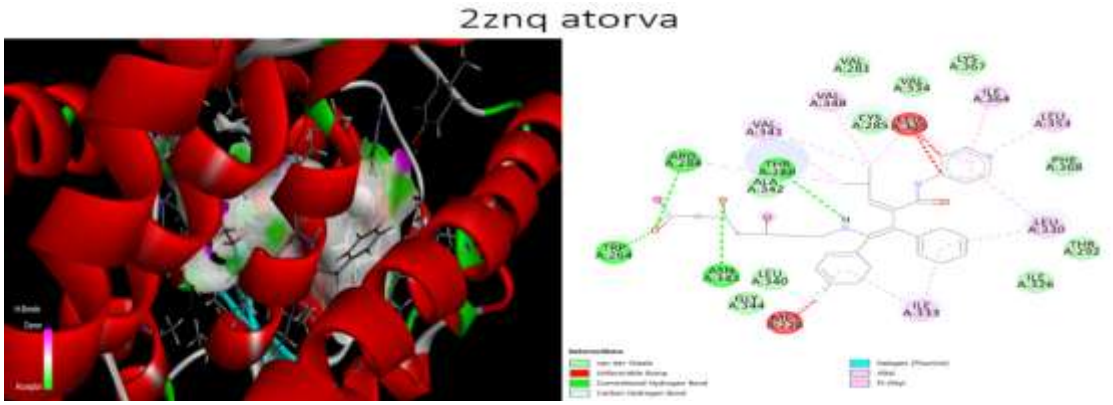

Figure 10: Docking image of the standard molecule Atorvastatin docked with 2znq Visualized throuth MVD and Biovia Visualizer software. A) 3D model. B) 2Dpose model.

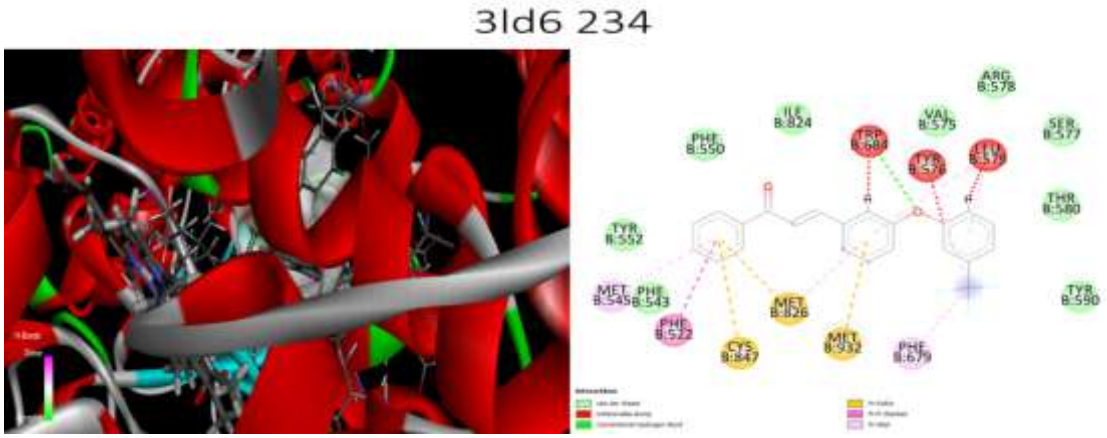

Figure 11: Docking image of the molecule code 234 docked with 3ld6 Visualized throuth MVD and Biovia Visualizer software. A) 3D model. B) 2Dpose model.

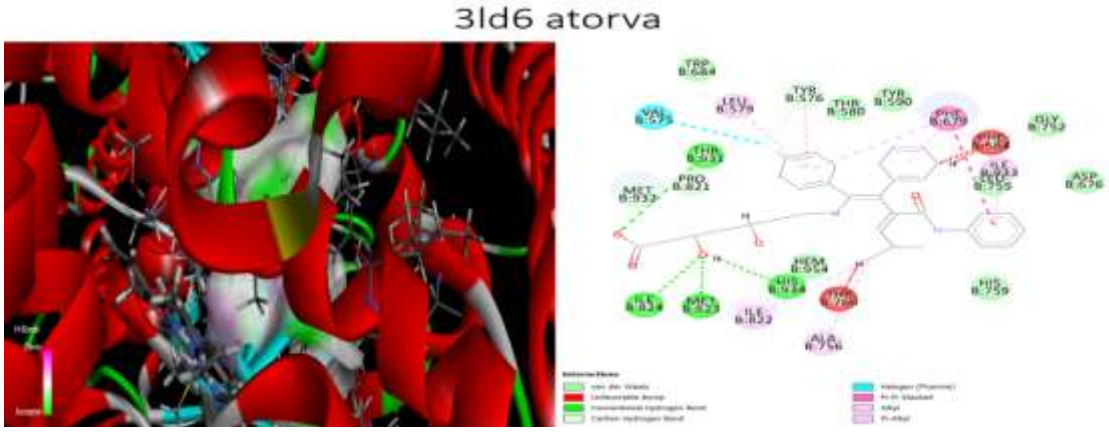

Figure 12: Docking image of the standard molecule Atorvastatin docked with 3ld6 Visualized throuth MVD and Biovia Visualizer software. A) 3D model. B) 2Dpose model.

Copyright © 2024 Authors

III. MATERIALS AND METHODS

1. **Materials:** The Protein Data Bank database was used to download and verify the protein structures of the chosen targets. Using Molegro virtual docker 6.0, the target was optimized and prepared. ChemDraw 8.0 was used to create the two-dimensional (2D) structures of the ligands.(19) The Chem3D Ultra 8.0 software was used to transform two-dimensional (2D) representations into three-dimensional (3D) ones, after which they were energetically re-duced using a technique built into the same program and stored as MDL moleFile (*.mol).

    - **Protein Preparation:** All receptors' protein structures were retrieved from the RCSB Protein Data Bank using the X-ray diffraction technique, and their resolutions are displayed in Figure 3.

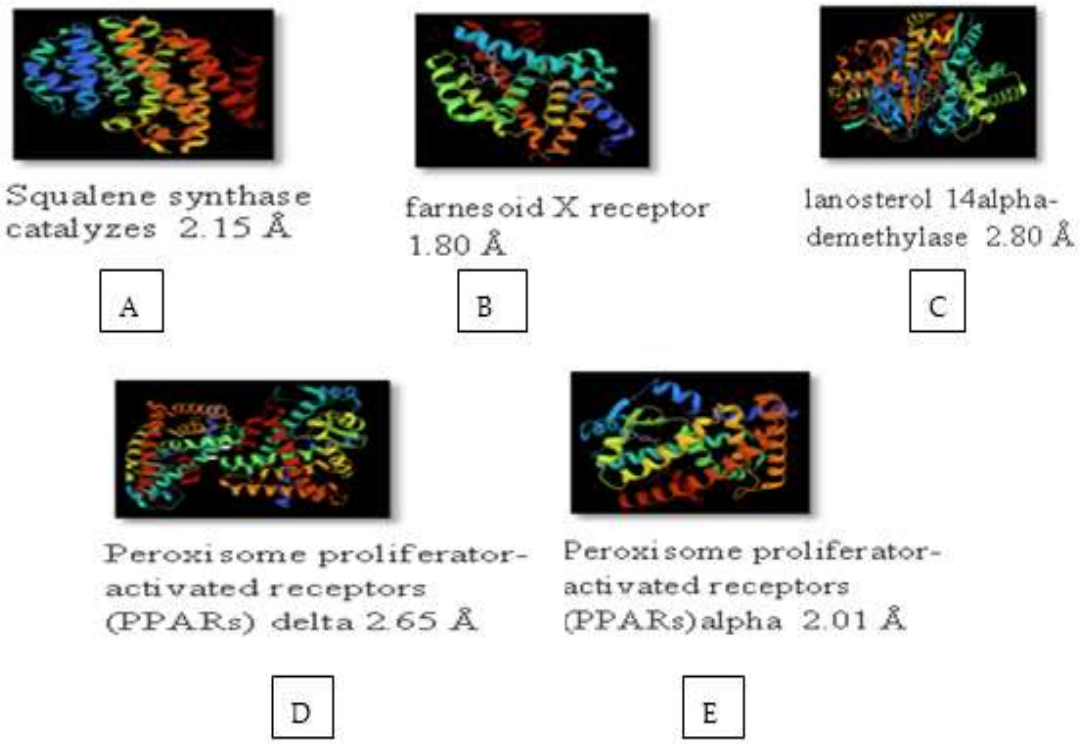

Figure 13

    - **Cavity Identification:** The grid-based cavity prediction technique was used to automatically identify the cavity with the possible binding site for ligands. The leftovers near the cavity were kept to a minimum. Only the side chains' torsion angles were changed during minimization; all other parameters, such as bond lengths and backbone atom locations, remained unchanged.(20)

2. **Import Molecules:** The ligands' 3D structures were loaded into MVD as *.mol files.

Copyright © 2024 Authors

Table 6: Details about Ligands Code with Structures

Ligands Code with Structures
444 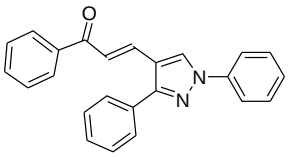
586 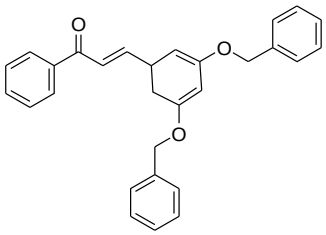
445 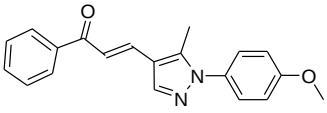
99 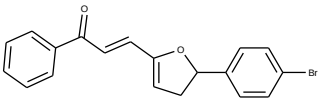
244 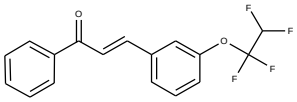
451 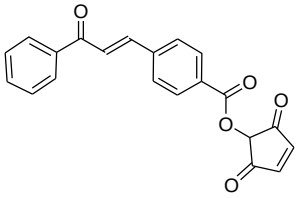
643 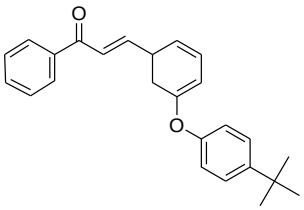
446 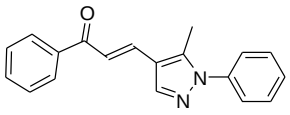
418 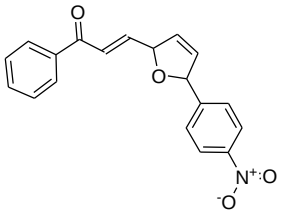
674 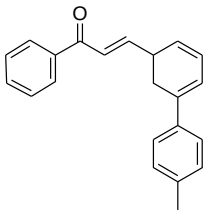
419 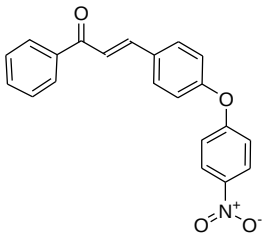
233 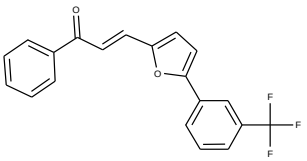
582 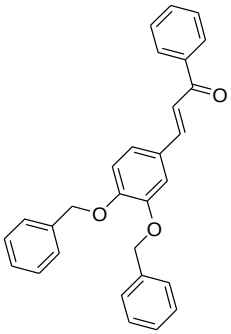
648 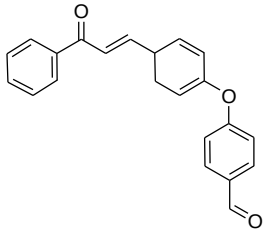
686 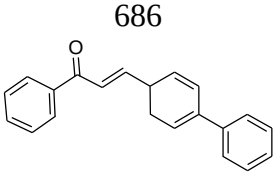
366	472	487

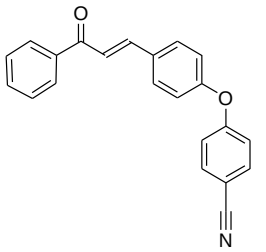

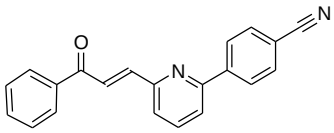

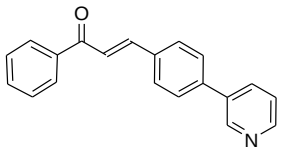

380

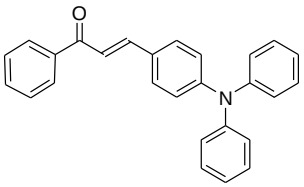

336

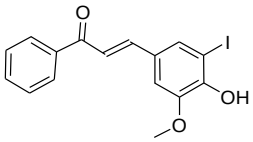

557

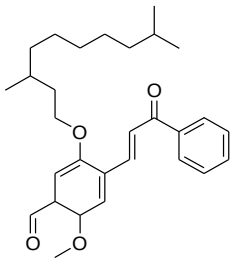

175

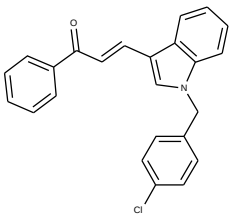

441

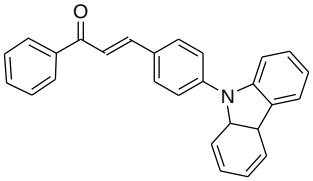

179

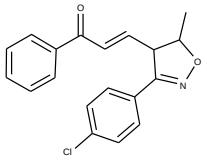

559

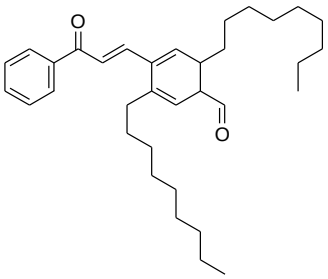

328

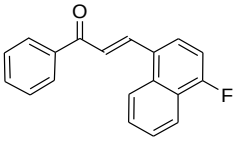

473

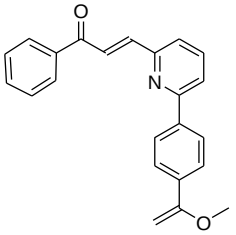

183

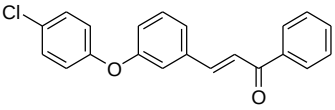

42

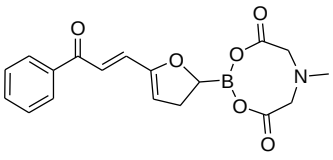

234

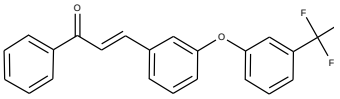

369

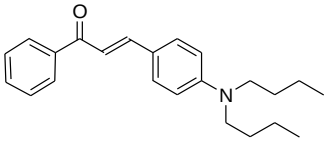

684

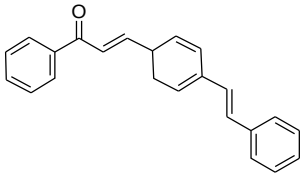

588

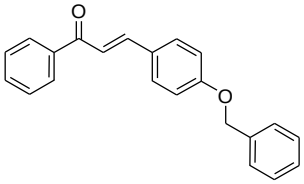

581

167

380

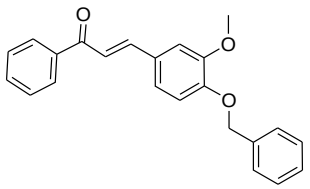
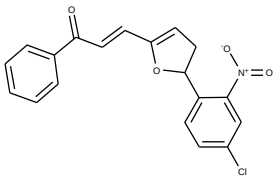
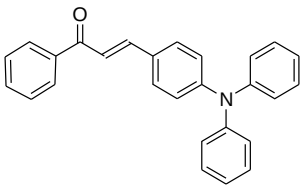

Table 7: Details about Ligands Code

S. No.	Ligand Code	IUPAC Names
1	444	(E)-1-phenyl-3-(1,3-diphenyl-1H-pyrazol-4-yl)prop-2-en-1-one
2	586	(2E)-3-(3,5-bis(benzyloxy)cyclohexa-2,4-dienyl)-1-phenylprop-2-en-1-one
3	445	(E)-3-(1-(4-methoxyphenyl)-5-methyl-1H-pyrazol-4-yl)-1-phenylprop-2-en-1-one
4	99	(2E)-3-(5-(4-bromophenyl)-4,5-dihydrofuran-2-yl)-1-phenylprop-2-en-1-one
5	244	(E)-3-(3-(1,1,2,2-tetrafluoroethoxy)phenyl)-1-phenylprop-2-en-1-one
6	451	2,5-dioxocyclopent-3-enyl 4-((E)-3-oxo-3-phenylprop-1-enyl)benzoate
7	643	(2E)-3-(5-(4-tert-butylphenoxy)cyclohexa-2,4-dienyl)-1-phenylprop-2-en-1-one
8	446	(E)-3-(5-methyl-1-phenyl-1H-pyrazol-4-yl)-1-phenylprop-2-en-1-one
9	418	(2E)-3-(2,5-dihydro-5-(4-nitrophenyl)furan-2-yl)-1-phenylprop-2-en-1-one
10	674	(2E)-1-phenyl-3-(5-p-tolylcyclohexa-2,4-dienyl)prop-2-en-1-one
11	419	(E)-3-(4-(4-nitrophenoxy)phenyl)-1-phenylprop-2-en-1-one
12	233	(E)-3-(5-(3-(trifluoromethyl)phenyl)furan-2-yl)-1-phenylprop-2-en-1-one
13	582	(E)-3-(3,4-bis(benzyloxy)phenyl)-1-phenylprop-2-en-1-one
14	648	(E)-4-((4-(3-oxo-3-phenylprop-1-en-1-yl)cyclohexa-1,5-dien-1-yl)oxy)benzaldehyde
15	686	(2E)-1-phenyl-3-(4-phenylcyclohexa-2,4-dienyl)prop-2-en-1-one
16	366	(E)-4-(4-(3-oxo-3-phenylprop-1-en-1-yl)phenoxy)benzonitrile
17	472	4-(6-((E)-3-oxo-3-phenylprop-1-enyl)pyridin-2-yl)benzonitrile
18	487	(E)-1-phenyl-3-(4-(pyridin-3-yl)phenyl)prop-2-en-1-one
19	380	(E)-3-(4-(diphenylamino)phenyl)-1-phenylprop-2-en-1-one
20	336	(E)-3-(4-hydroxy-3-iodo-5-methoxyphenyl)-1-phenylprop-2-en-1-one
21	557	3-(3,9-dimethyldecyloxy)-6-methoxy-4-((E)-3-oxo-3-phenylprop-1-enyl)cyclohexa-2,4-dienecarbaldehyde
22	175	(E)-3-(1-(4-chlorobenzyl)-1H-indol-3-yl)-1-phenylprop-2-en-1-one
23	441	(2E)-3-(4-(4bH-carbazol-9(8aH)-yl)phenyl)-1-phenylprop-2-en-1-one
24	179	(2E)-3-(3-(4-chlorophenyl)-4,5-dihydro-5-methylisoxazol-4-yl)-1-phenylprop-2-en-1-one
25	559	3,6-dinonyl-4-((E)-3-oxo-3-phenylprop-1-enyl)cyclohexa-2,4-dienecarbaldehyde

Copyright © 2024 Authors

26	328	(E)-3-(1-fluoronaphthalen-4-yl)-1-phenylprop-2-en-1-one
27	473	(E)-3-(6-(4-(1-methoxyvinyl)phenyl)pyridin-2-yl)-1-phenylprop-2-en-1-one
28	183	(E)-3-(3-(4-chlorophenoxy)phenyl)-1-phenylprop-2-en-1-one
29	42	2-(2,3-dihydro-5-((E)-3-oxo-3-phenylprop-1-enyl)furan-2-yl)-6-methyl-1,3,6,2-dioxazaborocane-4,8-dione
30	234	(E)-3-(3-(3-(trifluoromethyl)phenoxy)phenyl)-1-phenylprop-2-en-1-one
31	369	(E)-3-(4-(dibutylamino)phenyl)-1-phenylprop-2-en-1-one
32	684	(2E)-1-phenyl-3-(4-styrylcyclohexa-2,4-dienyl)prop-2-en-1-one
33	588	(E)-3-(4-(benzyloxy)phenyl)-1-phenylprop-2-en-1-one
34	581	(E)-3-(4-(benzyloxy)-3-methoxyphenyl)-1-phenylprop-2-en-1-one
35	167	(2E)-3-(5-(4-chloro-2-nitrophenyl)-4,5-dihydrofuran-2-yl)-1-phenylprop-2-en-1-one
36	380	(E)-3-(4-(diphenylamino)phenyl)-1-phenylprop-2-en-1-one

3. **Docking:** The backbone remained stiff throughout the docking simulation, but the side chains of amino acids near the discovered cavity were given the freedom to modify their torsional angles. The ligands were docked with the softening potentials during the simulation's docking process. The receptor was held stiff in this state, which is its default conformation. The side chains selected for reduction were then minimized with respect to the discovered posture after each ligand was docked. The ligand was reduced in energy when the side chains were repositioned. The conventional non-softened potentials were used to rearrange the side chains and minimize the ligand. As there can be a considerable reduction in the complexity of the docking search if fewer flexible torsions are set during the docking run, all flexible torsions in the ligand were made stiff during docking.

A Scoring Function's Parameters are:

- **Mol Dock Score:** The PLP (piecewise linear potential) scoring functions are the source of the MolDock scoring function (MolDock Score) that is employed by Molegro Vertual Docker. With a new hydrogen bonding term and new charge schemes, the MolDock scoring function enhances these scoring functions even further. The PLP (piecewise linear potential) scoring functions are the source of the MolDock scoring function (MolDock Score) that is employed by MVD. With a new hydrogen bonding term and new charge schemes, the MolDock scoring function enhances these scoring functions even further.The docking scoring function, Escore, is defined by the following energy terms: Escore = Einter + Eintra. Where, Einter is the ligand-protein interaction energy, Eintra is the internal energy of the ligand

- **Re-Rank Score:** The scoring function used for the re-ranking simulation was computationally more expensive than the scoring system for the docking simulation, but it is typically more effective at selecting the optimal posture from among numerous poses coming from the same ligand.(21) Although the re-rank score in MVD offers an estimate of the interaction's intensity, it is not calibrated in chemical units and does not account for complicated contributions (like entropy).(22) The re-rank score may

Copyright © 2024 Authors

be effective in rating various poses of the same ligand, but it may not be as effective in ranking various poses of different ligands.

IV. CONCLUSIONS

The structurally based drug design process involves the binding interaction of the ligand-protein. The 650 ligands of chalcone derivatives successfully demonstrated high binding affinity of MVD software towards the protein, Squalene synthase catalyzes, farnesoid X receptor, peroxisome proliferator-activated receptors (PPARs) alpha, peroxisome proliferator-activated receptors (PPARs) delta, and lanosterol 14alpha-demethylase. These ligands exhibited strong affinities for the target: 444, 419, 380, 366, and 234. According to computational docking studies, the drug chalcone derivatives displayed the highest binding affinity to the protein. The affinity for protein binding is displayed in tables 2, 3, 4, and 6. The substituted chalcone derivatives in the current study's docking investigations demonstrated strong binding affinities with the protein molecules, and the best substituted chalcone derivatives could be produced. In future we can design and synthesis some new and less toxic molecules using this docking results.

REFERENCES

[1] Aqeel MT, Ur-Rahman N, Khan AU, Ashraf Z, Latif M, Rafique H, et al. Antihyperlipidemic studies of newly synthesized phenolic derivatives: In silico and in vivo approaches. Drug Des Devel Ther. 2018;12:2443–53.

[2] S. LS, Raghu C, Arjun HA, Anantharaman P. In vitro and in silico inhibition properties of fucoidan against α-amylase and α-D-glucosidase with relevance to type 2 diabetes mellitus. Carbohydr Polym. 2019;209(1. Aqeel MT, Ur-Rahman N, Khan AU, Ashraf Z, Latif M, Rafique H, et al. Antihyperlipidemic studies of newly synthesized phenolic derivatives: In silico and in vivo approaches. Drug Des Devel Ther. 2018;12:2443–53. 2. Meng X-Y, Zhang H-X, Mezei M, Cui M. M):350–5.

[3] Shrivastava SK, Batham A, Sinha SK, Parida TK, Garabadu D, Choubey PK. Design, synthesis and evaluation of novel thiazolidinedione derivatives as anti-hyperglycemic and anti-hyperlipidemic agents. Med Chem Res. 2016;25(1. Aqeel MT, Ur-Rahman N, Khan AU, Ashraf Z, Latif M, Rafique H, et al. Antihyperlipidemic studies of newly synthesized phenolic derivatives: In silico and in vivo approaches. Drug Des Devel Ther. 2018;12:2443–53. 2. Meng X-Y, Zhang H-X, Mezei M, Cui M. M):2258–66.

[4] Othman R, Kiat TS, Khalid N, Yusof R, Newhouse EI, Newhouse JS, et al. Docking of noncompetitive inhibitors into dengue virus type 2 protease: Understanding the interactions with allosteric binding sites. J Chem Inf Model. 2008;48(1. Aqeel MT, Ur-Rahman N, Khan AU, Ashraf Z, Latif M, Rafique H, et al. Antihyperlipidemic studies of newly synthesized phenolic derivatives: In silico and in vivo approaches. Drug Des Devel Ther. 2018;12:2443–53. 2. Meng X-Y, Zhang H-X, Mezei M, Cui M. M):1582–91.

[5] Woods AD. Cholesterol levels. Nursing (Lond). 2010;40(8):31.

[6] Torres PHM, Sodero ACR, Jofily P, Silva-Jr FP. Key topics in molecular docking for drug design. Int J Mol Sci. 2019;20(18):1–29.

[7] Ramdhani D, Mustarichie R. Antihyperlipidemic Docking Study of Monascin and Ankaflavin Compounds From Monascus Purpureus With Some Targets Related With Hyperlipidemia. World J Pharm Res. 2021;10(2):28–35.

[8] Khedkar VM, Arya N, Coutinho EC, Shishoo CJ, Jain KS. Docking study of novel antihyperlipidemic thieno[2,3-d]pyrimidine; LM-1554, with some molecular targets related to hyperlipidemia - an investigation into its mechanism of action. Springerplus. 2014;3(1):1–31.

[9] Shukla P, Srivastava SP, Srivastava R, Rawat AK, Srivastava AK, Pratap R. Synthesis and antidyslipidemic activity of chalcone fibrates. Bioorganic Med Chem Lett. 2011;21(11):3475–8.

[10] Kar Mahapatra D, Asati V, Bharti SK. An updated patent review of therapeutic applications of chalcone derivatives (2014-present). Vol. 29, Expert Opinion on Therapeutic Patents. Taylor & Francis; 2019. 385–406 p.

Copyright © 2024 Authors

[11] Ouyang Y, Li J, Chen X, Fu X, Sun S, Wu Q. Chalcone derivatives: Role in anticancer therapy. Biomolecules. 2021;11(6):1–36.
[12] Rammohan A, Reddy JS, Sravya G, Rao CN, Zyryanov G V. Chalcone synthesis, properties and medicinal applications: a review. Vol. 18, Environmental Chemistry Letters. 2020. 433–458 p.
[13] Zhuang C, Zhang W, Sheng C, Zhang W, Xing C, Miao Z. Chalcone: A Privileged Structure in Medicinal Chemistry. Chem Rev. 2017;117(12):7762–810.
[14] Hassan RM, Aboutabl ME, Bozzi M, El-Behairy MF, El Kerdawy AM, Sampaolese B, et al. Discovery of 4-benzyloxy and 4-(2-phenylethoxy) chalcone fibrate hybrids as novel PPARα agonists with an-ti-hyperlipidemic and antioxidant activities: Design, synthesis and in vitro/in vivo biological evaluation. Bioorg Chem. 2021;115(October):2021–3.
[15] Kusumaningrum S, Budianto E, Kosela S, Sumaryono W, Juniarti F. The molecular docking of 1,4-naphthoquinone derivatives as inhibitors of Polo-like kinase 1 using Molegro Virtual Docker. J Appl Pharm Sci. 2014;4(11):47–53.
[16] Bitencourt-Ferreira G, de Azevedo WF. Molegro virtual docker for docking. Methods Mol Biol. 2019;2053:149–67.
[17] Binzet G. Eur opean J ournal of Chem istry. Eur J Chem. 2018;4(9):360–8.
[18] Manavi MA. In silico Study to Identification of Potential SARS-CoV-2 Main Protease Inhibitors: Virtual Drug Screening and Molecular Docking with AutoDock Vina and Molegro Virtual Docker. J Cell Mol Res. 2022;13(2):108–12.
[19] Julboev TA, Jizzakh State Pedagogical Institute Jizzakh U, Sultonov MM, Jizzakh State Pedagogical In-stitute Jizzakh U&, Komila Khudoyberdievna Abduvalieva Jizzakh State Pedagogical Institute Jizzakh U. Teaching chemistry computer software to students of chemistry in pedagogical higher education institutions. Eur J Res Reflect Educ Sci. 2021;9(2056–5852):23–8.
[20] Poleboyina PK, Pawar SC. Identification of Ethr Inhibitor Targeting Mycobacterium Tuberculosis : an Insight From Molecular Docking Study Insight From Molecular Docking Study. Asian J Pharm Clin Res. 2022;(March):145–52.
[21] Levin NMB, Pintro VO, Bitencourt-Ferreira G, de Mattos BB, de Castro Silvério A, de Azevedo WF. De-velopment of CDK-targeted scoring functions for prediction of binding affinity. Biophys Chem. 2018;235(April):1–8.
[22] Alabboud M, Javadmanesh A. In silico study of various antiviral drugs, vitamins, and natural substances as potential binding compounds with SARS-CoV-2 main protease. DYSONA - Life Sci. 2020;1(2):44–63.

Copyright © 2024 Authors